

Estimating Variations in SAR Calculations due to Within-Scan Patient Motion Using cGANs for Parallel RF Transmission at Ultrahigh Field MRI

Katherine Blanter, Alix Plumley, Shaihan Malik, Emre Kopanoglu

October 2023

Synopsis

Specific absorption rate (SAR), a proxy measure for tissue heating, is affected by patient motion. SAR safety factors during MRI scanning are intentionally overconservative. While designed to ensure patient safety, it impedes the utility of scanning with parallel-transmit (pTx) 7T MRI. We successfully used deep learning to predict the location of hot spots during head motion and applied them to a pTx design method which considers patient motion. We report that hot spots are overcalculated almost 1.5-fold when the degree of patient motion is not included compared to when it is.

Impact

Deep learning-estimated local specific absorption rate (SAR) variations caused by patient motion may be combined with within-scan motion detection and single-position, subject-specific models for personalized SAR predictions to create personalized SAR models for patients who cannot remain still.

Introduction

Transmitted radio frequency (RF) wavelengths for ultra-high field (UHF) MRI are often inhomogenous and cause an increase in the prevalence of tissue heating, or specific absorption rate (SAR).¹ RF inhomogeneity can be mitigated by parallel RF transmission (pTx) which can lead to localized SAR increases in unexpected locations. The literature shows that these effects worsen with unplanned patient motion.²⁻⁶ Previous work⁷ used conditional Generative Adversarial Networks (cGANs) to predict variations in B_1^+ from head motion. The current work applies a similar approach to predict variations in local SAR from head motion and validates them with a near-real-time pTx pulse redesign method.⁸

⁹ proposed using cGANs to predict the effects of rightward-posterior (R-P) motion on the magnitudes of 36-channel Q-matrices (8x8 channels of complex conjugates yielding 36 unique entries) derived from simulated head slabs. Predicting the phases of Q-matrices was unsuccessful, therefore a fraction of the pipeline was conceived. An algorithm¹⁰ was applied to recover phase information by creating real-valued 64-channel intermediary local SAR matrices (ilSAR). Last year's preliminary pipeline was rewritten, completed, and is presented here.

Methods

The dataset used was the same as the one generated for,² which consists of Sim4Life simulations (ZMT, Zurich, Switzerland) of body models (BMs) Billie, Duke, Fats, Ella and Glenn from the Virtual Population (IT'IS, Zurich, Switzerland)¹¹ at 34 positions (combinations of rightward-leftward (R-L):-20/-10/-5/0/5/10/20 and anterior-posterior (A-P):-10/-5/0/5/10). 8x8-channel Q-matrices were derived using the approach in.²

ilSAR were calculated with an algorithm¹⁰ designed to predict the power absorption consequence of a given RF pulse design (Figure 1).

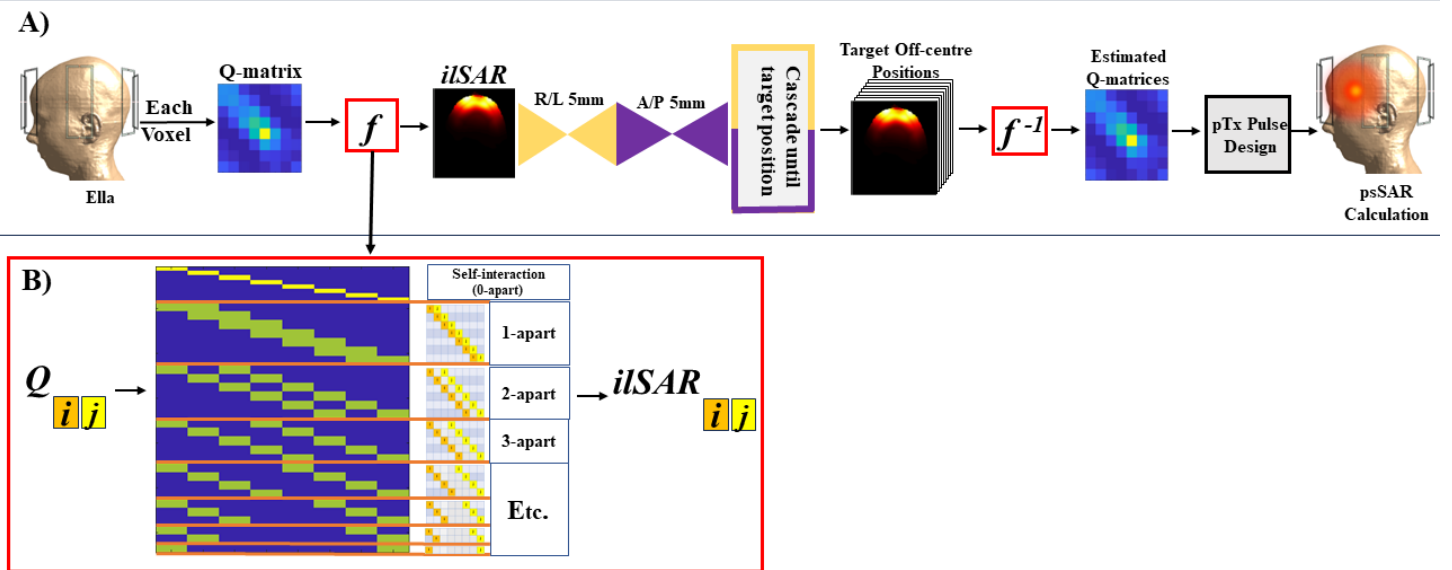


Figure 1: A) The preprocessing and evaluation workflow, where the first trained generator (trained on R/L/5/P 5mm translations) receives $iLSAR$ distributions at the center position before running sequentially until a determined translated position is reached (cascaded). The evaluated $iLSAR$ are inverted and introduced to the pulse-redesign protocol which yields peak spatial SAR calculation. B) The algorithm which calculated $iLSAR$ from Q-Matrices.

The cGAN was implemented in TensorFlow 2.4.1 and Python 3.7.11 on a NVIDIA DGX GPU in Linux. The architecture was identical to pix2pix,¹² excluding these parameters: epochs = 60; filter size = 1; strides = 1; a ReLU replaced with a leaky ReLU and no batch normalization in the generator network during downsampling. The data was normalized channel-wise, labeled with the degree of motion, and paired as given input and output $iLSAR$ distribution. A leave-one-out approach was used to create the training, validation, and testing data to prevent cross-talk (ie. TRAINING: Fats, Duke, and Billie; VALIDATION: Glenn; TESTING: Ella). To create the training pairs, the degrees of motion were paired both center-out and with displacement given an off-center reference (eg. R0 mm \rightarrow R5 mm and R5 mm \rightarrow R10 mm both represent R5 mm displacements). The training data contained 5,040 pairs for the P-A and 4,200 for the R-L networks. Testing was conducted using the same magnitude and direction of movement, and with the multiples of that trained magnitude direction and movement (ie. ‘cascading’ (figure 1)).

Network estimation quality was evaluated with L1 norm and averaged across slices per channel at each position by comparing ground truth (GT) voxel-wise with network estimated (NE) $iLSAR$. This was compared to L1 norm of motion-induced (MI) error (MIerr) (displaced GT simulations vs. centered $iLSAR$).

R-P $iLSAR$ estimations were remapped to Q-matrices¹³ and applied to a tailored near-real time pTx pulse redesign method⁸ (figure 1).

Results and Discussion

Figure 2 shows that the NE $iLSAR$ distributions resemble the GT across slices and movement types. 0-3 cascades are displayed from channel combinations yielding the worst error. MIerr maps (GT-centred) are more pronounced than the NE error (NEerr) maps (GT-NE).

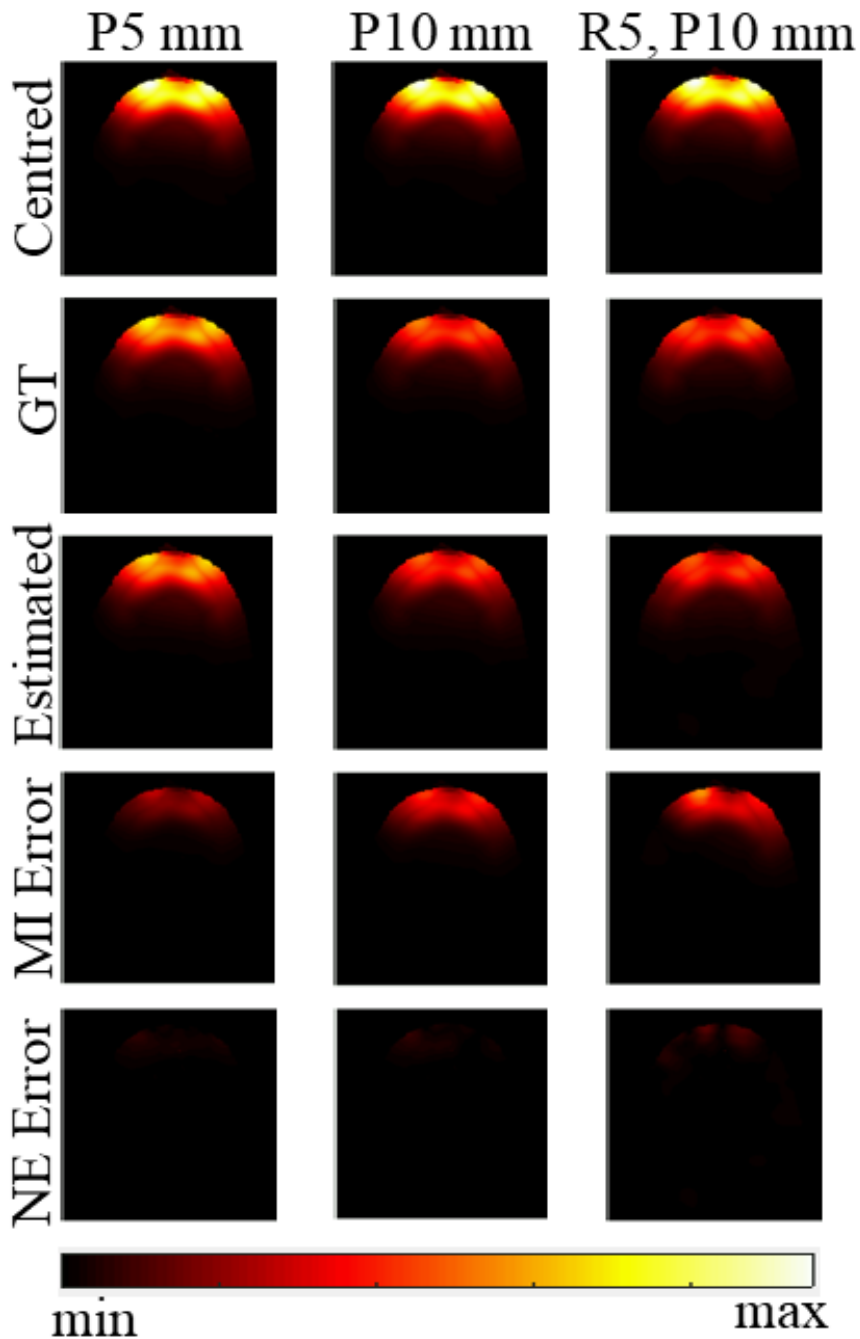


Figure 2: Each column contains maximum intensity projections along the z axis for the P5mm (0x cascades), P10mm (2x cascades), and R5, P10 mm (3x cascades) displacements arising from the channel interactions which yield the worst error. NEerr is far lower than MIerr.

Figure 3 plots the mean and maximum L1 errors across all pTx channel combinations and slices, per degree and direction of motion. In all cases, the mean and maximum MIerrs exceed NEerrs. Mean NEerr remains low throughout. While mean NEerr was 0.1%, never exceeding 0.7%, mean MIerr was 0.3%, reaching 1.5%.

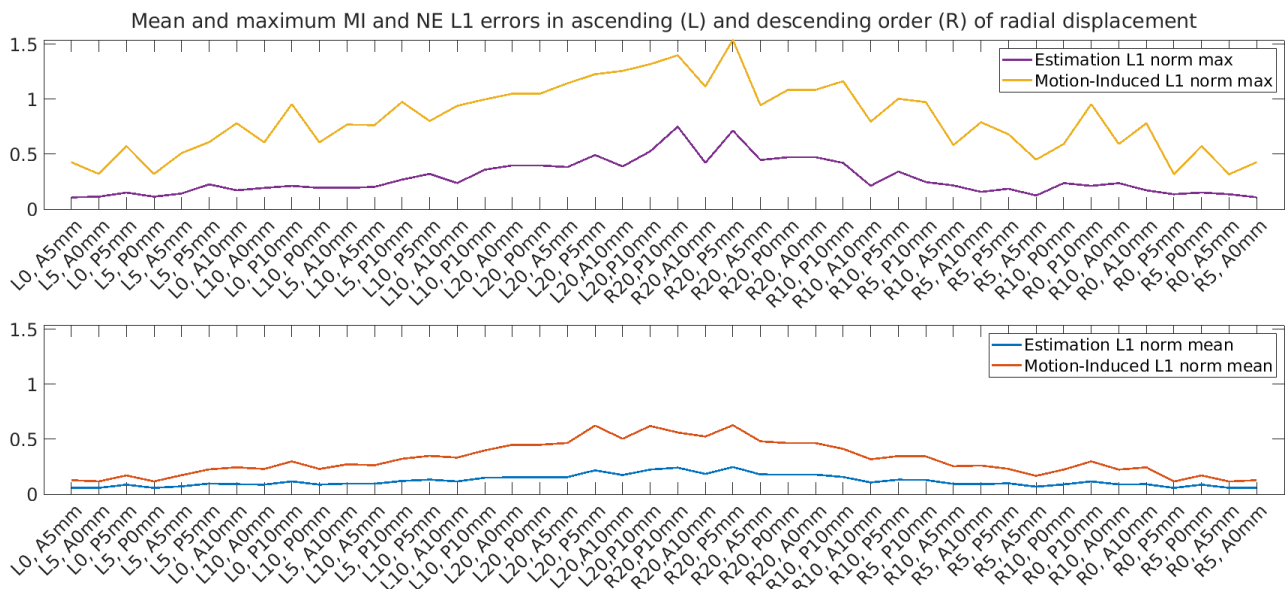


Figure 3: For all movement types, channels and slices, the mean and maximum NE L1 error was lower than MI L1 error. R and L are for rightward and leftward, respectively, and P and A are posterior anterior, respectively. Values are displayed in ascending(L)/descending(R) order of radial displacement from the centre.

Figure 4 displays the similarity between the R-P Q-matrices derived from the NE ilSAR distributions and the GT when including both as constraints in a near-real-time pTx design protocol. The resulting worst case underestimation is 2.5-fold when calculating psSAR with the centered BM (cBM), and 1.3-fold with the NE-BM. Using the cBM leads to 45% overcalculation, while using the NE-BM leads to 0.04% undercalculation.

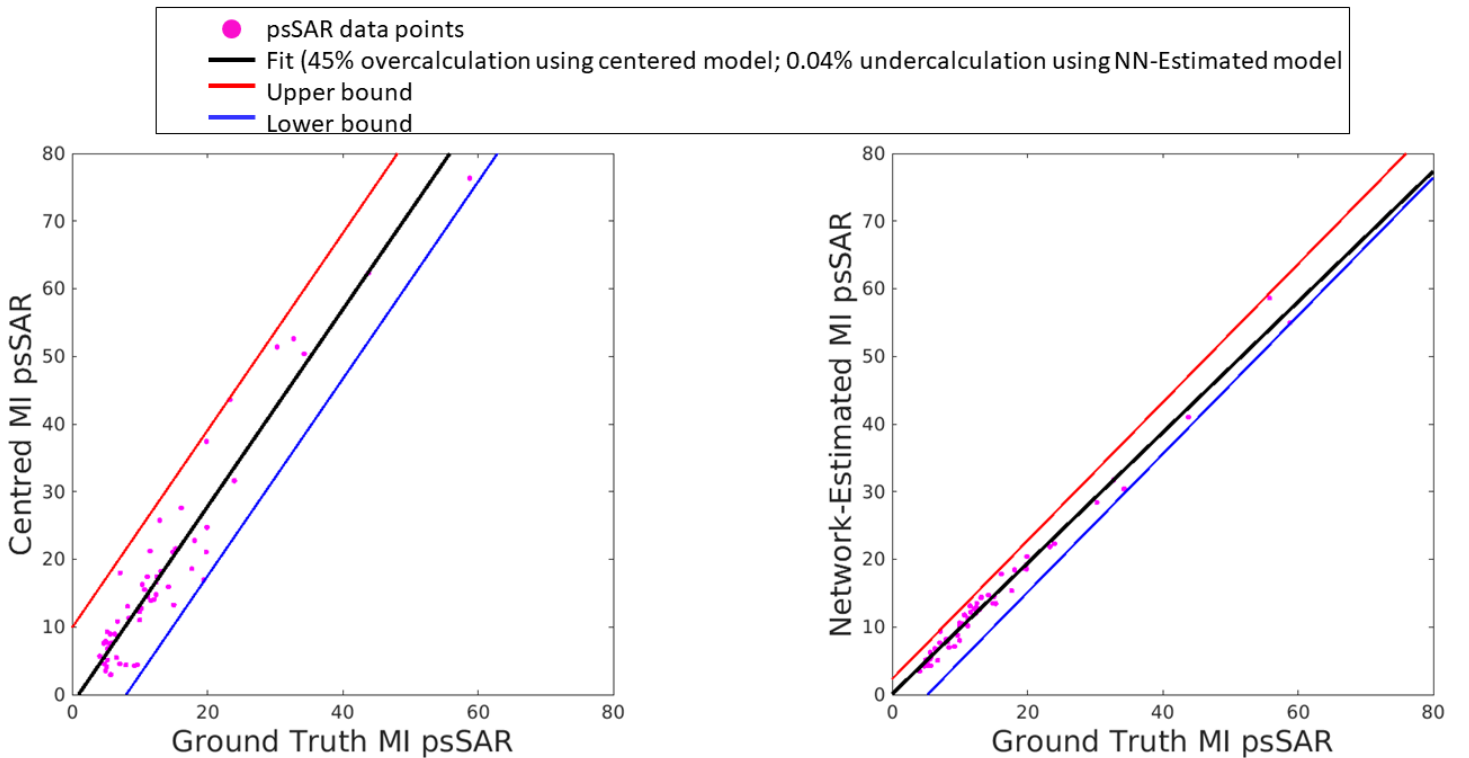


Figure 4: When used as real time pTx pulse design constraints, NE maps yield psSAR values nearly identical to those output when simulated GT maps are used, unlike the difference between centered and simulated GT values. The estimation error margin is one-third smaller when using the NE-BMs compared to the cBMs. Moreover, the slope of the black line indicates that using the cBMs leads to 45% psSAR overcalculation compared to 0.04% undercalculation when using the NE-BMs.

Conclusion

We have established a pipeline to estimate local SAR variations arising from head motion during 8-channel pTx at UHF-MRI. Since our NE and GT ilSAR distributions are compatible, this approach can be developed for near-real-time pTx with revised, less overconservative safety factors. Future work will expand the pipeline to include yaw and 2mm degrees of motion.

Acknowledgements

This project was supported in part by the Wellcome Trust [204824/Z/16/Z], Welsh Government [Wales Data Nation Accelerator project], and EPSRC [Doctoral Training Program].

References

- ¹ Frank Seifert, Gerd Wübbeler, Sven Junge, Bernd Ittermann, and Herbert Rinneberg. Patient safety concept for multichannel transmit coils. *Journal of Magnetic Resonance Imaging*, 26:1315–1321, 11 2007.
- ² Emre Kopanoglu, Cem M. Deniz, M. Arcan Erturk, and Richard G. Wise. Specific absorption rate implications of within-scan patient head motion for ultra-high field mri. *Magnetic Resonance in Medicine*, 84:2724–2738, 11 2020.
- ³ Emre Kopanoglu. Actual patient position versus safety models: Specific absorption rate implications of initial head position for ultrahigh field magnetic resonance imaging. *NMR in Biomedicine*, 5 2022.
- ⁴ Morgane Le Garrec, Vincent Gras, Marie France Hang, Guillaume Ferrand, Michel Luong, and Nicolas Boulant. Probabilistic analysis of the specific absorption rate intersubject variability safety factor in parallel transmission mri. *Magnetic Resonance in Medicine*, 78:1217–1223, 9 2017.
- ⁵ Amer Ajanovic, Joseph V Hajnal, and Shaihan Malik. Positional sensitivity of specific absorption rate in head at 7t. volume 4251, 2020.

- ⁶ Amer Ajanovic, Joseph V Hajnal, Raphael Tomi-Tricot, and Shaihan Malik. Motion and pose variability of sar estimation with parallel transmission at 7t. volume 2487, 2021.
- ⁷ Alix Plumley, Luke Watkins, Matthias Treder, Patrick Liebig, Kevin Murphy, and Emre Kopanoglu. Rigid motion-resolved prediction using deep learning for real-time parallel-transmission pulse design. *Magnetic Resonance in Medicine*, 87:2254–2270, 5 2022.
- ⁸ Emre Kopanoglu. Near real-time parallel-transmit pulse design. 2018.
- ⁹ Emre Kopanoglu Katherine Blanter, Alix Plumley. Shaihan Malink. Towards applying deep learning to predict rigid motion-induced changes in q-matrices from uhf-mri ptx simulations. 2023.
- ¹⁰ Yudong Zhu, Leeor Alon, Cem M. Deniz, Ryan Brown, and Daniel K. Sodickson. System and sar characterization in parallel rf transmission. *Magnetic Resonance in Medicine*, 67:1367–1378, 5 2012.
- ¹¹ Honegger Katharina Zefferer Marcel Neufeld Esra Oberle Michael Szczerba Dominik Kuster Niels Kainz Wolfgang Guag Joshua W Hahn Eckhart G Rascher Wolfgang Janka Rolf Bautz Werner Chen Ji Shen Jianxiang Kiefer Berthold Schmitt Peter Hollenbach Hans-Peter Christ, Andreas and Anthony Kam. The virtual family-development of surface-based anatomical models of two adults and two children for dosimetric simulations, Jan 2010.
- ¹² Phillip Isola, Jun-Yan Zhu, Tinghui Zhou, Alexei A Efros, and Berkeley Ai Research. Image-to-image translation with conditional adversarial networks, 2017.
- ¹³ Arian Beqiri, JV Hajnal, and SJ Malik. Local q-matrix computation for parallel transmit mri using optimal channel combinations. In *Proceedings of the 24th Annual Meeting of ISMRM, Singapore*, page 3658, 2016.